Transportation Research Part C xxx (2016) xxx–xxx

Contents lists available at ScienceDirect

Transportation Research Part C

journal homepage: www.elsevier.com/locate/trc

Optimal speed advisory for connected vehicles in arterial roads and the impact on mixed traffic

Nianfeng Wan [a,*], Ardalan Vahidi [a], Andre Luckow [b]

[a] Department of Mechanical Engineering, Clemson University, Clemson, SC, United States
[b] BMW Group Information Technology Research Center, Greenville, SC, United States

ARTICLE INFO

Article history:
Received 16 June 2015
Received in revised form 18 January 2016
Accepted 24 January 2016
Available online xxxx

Keywords:
Speed advisory system
Connected vehicle
Optimal control
Traffic signals
Fuel consumption
Arterial traffic

ABSTRACT

Connected Vehicles (CV) equipped with a Speed Advisory System (SAS) can obtain and utilize upcoming traffic signal information to manage their speed in advance, lower fuel consumption, and improve ride comfort by reducing idling at red lights. In this paper, a SAS for pre-timed traffic signals is proposed and the fuel minimal driving strategy is obtained as an analytical solution to a fuel consumption minimization problem. We show that the minimal fuel driving strategy may go against intuition of some people; in that it alternates between periods of maximum acceleration, engine shut down, and sometimes constant speed, known in optimal control as bang-singular-bang control. After presenting this analytical solution to the fuel minimization problem, we employ a sub-optimal solution such that drivability is not sacrificed and show fuel economy still improves significantly. Moreover this paper evaluates the influence of vehicles with SAS on the entire arterial traffic in micro-simulations. The results show that SAS-equipped vehicles not only improve their own fuel economy, but also benefit other conventional vehicles and the fleet fuel consumption decreases with the increment of percentage of SAS-equipped vehicles. We show that this improvement in fuel economy is achieved with a little compromise in average traffic flow and travel time.

1. Introduction

Connected Vehicles (CV) are able to access and share information wirelessly with each other and with the infrastructure in real time through vehicle-to-vehicle and vehicle-to-infrastructure communication protocols. Informed by this rich "ambient" data, connected vehicles can adjust their movements in coordination with other vehicles and traffic control systems and enhance their safety, energy efficiency, and mobility. Research on the technology and applications of connected vehicles has been ongoing for many years around the world; an example is the large testbed with thousands of connected vehicles that has been deployed in the city of Ann Arbor, Michigan (Krueger and Fehr, 2013). In 2014, the U.S. Department of Transportation (DOT) issued advance notice of proposed rule-making to begin implementation of vehicle-to-vehicle communications technology in new vehicles (Howden, 2015). Therefore it is expected that in near future new vehicles in the US have the communication capability to communicate with each other and perhaps with intelligent infrastructure such as traffic signals.

A large body of research has been done on developing driving strategies that improves fuel economy. For example in Li et al. (2015a) the authors proposed a fuel optimized operating strategy, they concluded that the optimal operating strategy is periodic because of the S-shaped engine fueling rate. In Eben Li et al. (2013), the authors propose a headway control

* Corresponding author.

http://dx.doi.org/10.1016/j.trc.2016.01.011
0968-090X/

algorithm to reduce fuel. In Hellström et al. (2010, 2009), the authors propose look-ahead control algorithms which take upcoming road topography into account to reduce fuel consumption. These approaches assume that vehicles are not communicating among each other. With CV technologies, new approaches are emerging rapidly. In Bhavsar et al. (2014), the authors propose energy saving strategies for plug-in hybrid electric vehicles using upcoming traffic signal timing and headway information.

A Speed Advisory System (SAS) that aids in reducing idling near traffic signals is one of the applications of CV technology, which has been proposed by our research group (Asadi and Vahidi, 2009, 2011; Mahler and Vahidi, 2014) and various other researchers across the world (Koukoumidis et al., 2011; Mandava et al., 2009; Rakha and Kamalanathsharma, 2011; Wollaeger et al., 2012). Vehicles equipped with a Speed Advisory System (SAS) can utilize upcoming traffic signal information predictively and manage their speed in advance to reduce idling at red lights. SAS relies on vehicle connectivity to obtain traffic Signal Phase and Timing (SPaT). The technology for transmitting traffic signal information to subscribing vehicles has been demonstrated in several research projects (Koukoumidis et al., 2011; Xia et al., 2012). The SPaT information may be directly transmitted to vehicles within range using Dedicated Short Range Communications (DSRC) technology (Koukoumidis et al., 2011) or may become available by the traffic control center through cellular and Wi-Fi networks. Alternative means of inferring SPaT information via on-board cameras (Koukoumidis et al., 2011) and via crowd-sourcing (Fayazi et al., 2015) have also been proposed.

Motion planning or trajectory planning problems can be formulated as optimal control problems (Katrakazas et al., 2015). Past research has formulated the speed advisory problem as optimal control problems and obtained the optimal speed trajectory. In Asadi and Vahidi (2011) and Kamal et al. (2010, 2013) Model Predictive Control (MPC) approaches have been used to obtain near optimal trajectories while considering traffic signals. In He et al. (2015) the authors propose to obtain speed trajectories considering queue pattern and signal timings. In Mahler and Vahidi (2014), Kamalanathsharma and Rakha (2013), Kamalanathsharma et al. (2015), and Ozatay et al. (2014), the authors propose Dynamic Programming (DP) approaches to solve the optimal control problem. Unfortunately, these methods are costly in terms of CPU and memory use and often cannot be executed in real time. In Ozatay et al. (2012), the authors use a linearized model of a vehicle's longitudinal dynamics and solved the fuel minimization problem analytically with given boundary conditions. This analytical method is computationally less expensive and by which the approach proposed in our paper is inspired. The solution we propose maintains the nonlinearities in vehicle dynamics, relaxes the boundary conditions to the minimum required information, and solves the optimal control problem relying on Pontryagin's Minimum Principle (PMP) and kinematic constraints. We show that the optimal solution requires switching between maximum engine torque (boost) and engine shut-down (glide) and occasionally includes a period of constant speed (sustain). Similar conclusions can be found in Li and Peng (2011) and Li et al. (2012). We then argue that the resulting speed profile, while fuel optimal, is uncomfortable to drivers and may also be disruptive to surrounding traffic. We then resort to modified suboptimal speed profiles and still show improvement in fuel economy as a result of avoiding red lights.

Equipped with analytical solutions, we then evaluate the impact on fuel economy in mixed traffic conditions. SAS can significantly reduce energy consumption of individual vehicles and improves their ride comfort, yet it decreases the average speed of equipped vehicles and increases their travel time. It is not difficult to analyze the effect on each equipped vehicle itself (Asadi and Vahidi, 2011; Mahler and Vahidi, 2014; Rakha and Kamalanathsharma, 2011; Boyle and Mannering, 2004; Manzie et al., 2007). However, the SAS technology is unlikely to be implemented in every vehicle in the near future. Therefore it is essential to evaluate the influence of equipped vehicles on other vehicles in mixed traffic flow. There are many papers aiming at evaluating the impact of adaptive cruise control in mixed traffic (Kesting et al., 2010; Ioannou and Stefanovic, 2005), or the impact of vehicle-infrastructure cooperation (Farah et al., 2012). However, to the authors' best knowledge, there are few papers discussing the impact of SAS on mixed traffic for multiple intersections. For instance in Kamalanathsharma et al. (2015) and in Xia et al. (2013) the authors evaluate the influence of eco-driving or eco-speed control only on vehicles equipped with such a system, or only on the surrounding traffic. Another example in Mensing et al. (2014) only discusses impacts of eco-driving on ego-vehicle's pollutant emission and fuel consumption. In Boyle and Mannering (2004) the authors only discuss impacts of speed advisory to driving behavior. In this paper, we evaluate the influence of SAS-equipped vehicles on each other as well as on conventional vehicles. Moreover, in this paper we evaluate the system when traveling across multiple intersections.

It is currently prohibitively difficult to do in the field experiments of a large number of connected vehicles in mixed traffic. Therefore it is necessary to choose a simulation tool to conduct simulations under different traffic situations. In this paper we use the microscopic traffic simulation tool *Paramics*. Paramics is able to simulate a large number of vehicles in a complex traffic network. Moreover, it is easy to set percentages of different types of vehicles and adjust traffic demands. A direct result is measurement of instantaneous speed and acceleration values that influence driving comfort as well as fuel consumption. Vehicles equipped with SAS aim to avoid sharp braking and/or stopping at traffic signals, which improves their fuel efficiency. We will use a fuel consumption model to calculate the fuel economy of each vehicle based on its velocity and acceleration profile. From velocity trajectories we also evaluate travel time of each vehicle. In Paramics it is possible to install virtual sensors to also measure traffic flow. We use these virtual measurements to evaluate the side effects of the proposed SAS technology.

The rest of this paper is organized as follows: Section 2 presents the optimal control framework for obtaining analytical solutions for the optimal speed trajectory of individual vehicles. Section 3 introduces the simulation environment, parameters, and various test setups. The results are summarized in Section 4 followed by conclusions in Section 5.

Please cite this article in press as: Wan, N., et al. Optimal speed advisory for connected vehicles in arterial roads and the impact on mixed traffic. Transport. Res. Part C (2016), http://dx.doi.org/10.1016/j.trc.2016.01.011

2. Optimal control formulation of SAS

In SAS the goal is to calculate a reference speed profile based on ego vehicle's position, speed, and upcoming Signal Phase and Timing (SPaT) such that if the vehicle follows this speed trajectory, it consumes the least amount of fuel. Often the vehicle is guided to pass the intersection when the light is green. This is due to the fact that stop-and-go motion requires more energy than cruising and should be reduced as much as possible. In this section we formulate this problem as an optimal control problem and present an analytical solution for it.

2.1. The vehicle model

The vehicle longitudinal dynamics is needed and can be written as (Vahidi et al., 2005):

$$m\dot{v} = \frac{T_e}{r_g} - \frac{1}{2}\rho_a A C_D v^2 - mg(\mu cos\theta + sin\theta) - F_b \tag{1}$$

where m is mass of the vehicle and includes powertrain inertial effects, v is forward velocity, T_e is the engine torque at the flywheel, F_b is the braking force generated at the tire contact point with the road. The parameter r_g is the wheel radius divided by total gear ratio. Air density is ρ_a, A is vehicle front area, C_D is aerodynamic drag coefficient, and μ is the rolling friction coefficient. The road slope angle is θ and in this paper it is assumed to be a constant over time to simplify the analytical derivations. We also assume the gear ratio and therefore r_g remain constant; this assumption enables us to generate analytical solutions and is valid during a large part of city cruising when the vehicle is in a fixed gear.[1]

The longitudinal dynamics in (2) can be rewritten in the following form after dividing both sides by m:

$$\dot{v} = u_e - C_1 v^2 - C_2 - u_b \tag{2}$$

where $u_e = \frac{T_e}{m r_g}$ is the vehicle acceleration contributed by engine torque, $u_b = \frac{F_b}{m}$ is the vehicle deceleration due to braking force, and $C_1 = \frac{1}{2}\frac{\rho_a A C_D}{m}$ and $C_2 = g(\mu cos\theta + sin\theta)$ are constants, where we assumed that road grade is time-invariant.

The fuel minimization problem can be cast as an optimal control problem, in which the vehicle's position x and velocity v are the dynamic states and the control inputs are u_e and u_b. Note that the braking force should be zero while the engine torque is positive, and vice versa. And we intuitively know that the minimum fuel solution will avoid braking when possible. Therefore we can separate the engine engaged case from the braking applied case, and discuss them respectively.

Based on Eq. (2) and when braking is not applied, we have the following state-space equations:

$$\begin{cases} \dot{x} = v \\ \dot{v} = u_e - C_1 v^2 - C_2 \end{cases} \tag{3}$$

The upper bound on control input u_e^{max} corresponds to the maximum engine torque T_e^{max} and the lower bound $u_e^{min} = 0$ corresponds to zero engine torque (engine shut-off). Note that maximum engine torque depends on the operating point of the engine. However since u_e^{max} is the maximum traction force at wheel, we assume that a fixed maximum value is always achievable by selection of gear and engine torque. The upper bound on the velocity is the maximum speed limit of the road and the lower bound is such that the vehicle does not significantly block the traffic.

Besides the vehicle dynamics model, a fuel consumption estimation model is also needed. In this paper, the fuel consumption estimation model is adopted from Kamal et al. (2011), where the authors sampled sufficient data from a passenger size vehicle and fit into third order polynomial curves that approximate the relation between fuel consumption rate and velocity and acceleration. In this model the fuel consumption rate $\dot{m}_f$, during positive acceleration and constant speed cruising is estimated by:

$$\dot{m}_f = \alpha_0 + \alpha_1 v + \alpha_2 v^2 + \alpha_3 v^3 + (\beta_0 + \beta_1 v + \beta_2 v^2)a$$

where a is the vehicle acceleration and α_i and β_i are model parameters. The parameter values is presented later in Table 1. Note that this fuel consumption model assumes that the road gradient is zero. When the acceleration is negative, we assume that the engine is idling and consuming a minimal constant fuel rate α_0.[2] To summarize, we employ the following model for fuel consumption rate:

$$\dot{m}_f = \begin{cases} \alpha_0 + \alpha_1 v + \alpha_2 v^2 + \alpha_3 v^3 + (\beta_0 + \beta_1 v + \beta_2 v^2)a, & a \geqslant 0 \\ \alpha_0, & a < 0 \end{cases} \tag{4}$$

[1] One can consider the gear choice as an extra degree of freedom for energy optimization which introduces a discrete optimization variable and almost certainly requires a numerical optimization procedure. Alternatively and more realistically one can rely on the existing gear shift logic of a vehicle and augment it either in the longitudinal dynamics model in Eq. (1) or incorporate it in the fuel economy model. In either case, the problem will not lend itself to an analytical solution such as the one presented in this paper and a numerical solution may be unavoidable.

[2] Later in this paper we show that the optimal strategy is to either run the engine at maximum torque, zero torque, such that the vehicle is at a constant speed. Therefore under these conditions, negative vehicle acceleration can only correspond to engine idle/shut-off which justifies the assumption of minimal constant fuel rate.

Please cite this article in press as: Wan, N., et al. Optimal speed advisory for connected vehicles in arterial roads and the impact on mixed traffic. Transport. Res. Part C (2016), http://dx.doi.org/10.1016/j.trc.2016.01.011

Table 1
Values of vehicle model parameters.

Coefficient	Value	Unit	Coefficient	Value	Unit
m	1200	kg	A	0.25	m^2
C_D	0.35	–	g	9.8	m/s^2
ρ_a	1.184	kg/m^3	μ	0.015	–
u_e^{max}	2.5	m/s^2	u_b^{max}	2.9	m/s^2
v_{max}	80	km/h	v_{min}	10	km/h
α_0	0.1569	$\frac{mL}{s}$	β_0	0.07224	$\frac{mL\,s}{m}$
α_1	2.450×10^{-2}	$\frac{mL}{m}$	β_1	9.681×10^{-2}	$\frac{mL\,s^2}{m^2}$
α_2	-7.415×10^{-4}	$\frac{mL\,s}{m^2}$	β_2	1.075×10^{-3}	$\frac{mL\,s^3}{m^3}$
α_3	5.975×10^{-5}	$\frac{mL\,s^2}{m^3}$			

2.2. Fuel consumption minimization

The vehicles equipped with SAS can uni-directionally receive the relevant signal information via DSRC. Alternatively equipped vehicles may subscribe to each upcoming light via a cellular network and receive updated SPaT information from the signal. The distance between the light and current vehicle can be estimated from the vehicle's GPS coordinates and traffic light information. Through V2I communication, the information such as current phase, time left in the current phase, phase duration and cycle length of the upcoming traffic signal also become available. Therefore, several time windows that the vehicle can pass at green can be calculated as illustrated schematically in Fig. 1. In this paper it is assumed that the vehicle calculates the first feasible time to pass during green, given the road speed limits. In the future it may be possible for intelligent traffic signals to reserve and allocate a time to each subscribing vehicle to pass during green (Au et al., 2015).

Given a start time t_0 and a target time t_f to arrive at the signal, our objective is to find the fuel minimal velocity profile and corresponding control inputs for the vehicle. In other words the goal is to find the control input that minimizes the following cost function:

$$J = \int_{t_0}^{t_f} \dot{m}_f \, dt \tag{5}$$

subject to the state dynamics in Eq. (3) and the control input constraint that $0 \leqslant u_e \leqslant u_e^{max}$. This is a calculus of variation problem and one can obtain necessary conditions for optimality in the form of ordinary differential equations. In control theory these necessary conditions for optimality are described by Pontraygin's Minimum Principle (PMP) (Kirk, 2012). According to PMP, first the *Hamiltonian* is constructed as the sum of the integrand in (5) and the right side of the state equations in (3) multiplied by Lagrange multipliers $\lambda_i(t)$, also referred to as *costates*:

$$H = \dot{m}_f + \lambda_1(t)v + \lambda_2(t)(u_e(t) - C_1 v^2 - C_2) \tag{6}$$

PMP states that the optimal input trajectory $u_e^*(t)$ and the corresponding optimal state and co-state trajectories must minimize the Hamiltonian. Combining Eqs. (3), (4), and (6), we observe that in our problem the Hamiltonian is an affine function of the control input u_e; therefore the partial derivative,

$$H_u = \frac{\partial H}{\partial u_e} = \beta_0 + \beta_1 v + \beta_2 v^2 + \lambda_2 \tag{7}$$

does not contain the control input term u_e. This indicates that the optimal control switches between control boundaries, 0 and u_e^{max}, depending on the sign of H_u. If $H_u = 0$ for an interval in time, the system is said to be on a singular arc and the control will assume a value between the upper and lower constraints; in this paper we refer to it as u_e^{sing}. In other words,

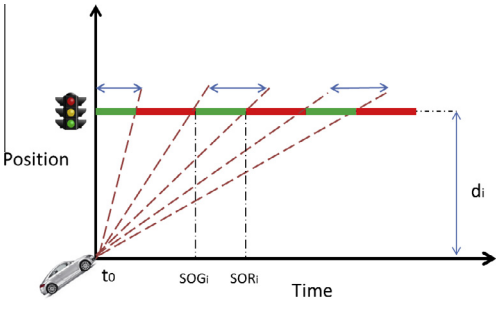

Fig. 1. Schematics of the speed advisory system.

Please cite this article in press as: Wan, N., et al. Optimal speed advisory for connected vehicles in arterial roads and the impact on mixed traffic. Transport. Res. Part C (2016), http://dx.doi.org/10.1016/j.trc.2016.01.011

$$u_e^* = \begin{cases} u_e^{max} & \text{if}(\beta_0 + \beta_1 v + \beta_2 v^2 + \lambda_2) < 0 \\ 0 & \text{if}(\beta_0 + \beta_1 v + \beta_2 v^2 + \lambda_2) > 0 \\ u_e^{sing} & \text{if}(\beta_0 + \beta_1 v + \beta_2 v^2 + \lambda_2) = 0 \end{cases} \tag{8}$$

which is referred to as bang-singular-bang control.[3] The PMP necessary conditions also describe the dynamics of the co-states as $\dot{\lambda_1} = -H_x$ and $\dot{\lambda_2} = -H_v$, therefore:

$$\begin{cases} \dot{\lambda_1} = -\frac{\partial H}{\partial x} = 0 \\ \dot{\lambda_2} = -\frac{\partial H}{\partial v} = -[\alpha_1 + 2\alpha_2 v + 3\alpha_3 v^2 + (\beta_1 + 2\beta_2 v)(u_e - C_1 v^2 - C_2) \\ \qquad\qquad + (\beta_0 + \beta_1 v + \beta_2 v^2)(-2C_1 v) + \lambda_1 - 2C_1 \lambda_2 v] \end{cases} \tag{9}$$

In general the dynamics of co-states must be tracked because the optimal control input will depend on them. State dynamics in Eq. (3), the co-state dynamics in Eq. (9) together with Eq. (8) form the necessary conditions for optimality. To solve the 4 differential equations in (3) and (8), which are in general coupled, 4 boundary conditions are needed. Here $x(t_0)$, $v(t_0)$, and $x(t_f)$ are specified. We can either constrain the velocity at t_f which provides an additional boundary condition or leave it open; in the latter case the value of $\lambda_2(t_f)$ will be fixed and known according to the theory of optimal control (Kirk, 2012). This is a two-point boundary value problem, because the boundary conditions are split at both ends, and in general is very hard to solve analytically. Fortunately the special structure of the problem in this paper (bang-singular-bang control and mild coupling in dynamics) allows us to obtain an analytical solution as discussed next.

2.3. Analytical solution for minimum fuel control

As shown in Eq. (8), the optimal engine input alters between its two extreme values if the inequality conditions hold. When the equality condition is satisfied for an extended interval, the system is said to be moving on a singular arc, and the optimal control input could vary between u_e^{max} and zero. Further analysis is needed to verify the existence of a singular arc and to obtain the corresponding optimal control input $u_e^{sing}(t)$. Because this analysis is outside of the scope of this paper, we present it in Appendix A.

The conclusion in Appendix A is that a singular arc could exist (albeit occasionally and at very low speeds). On a singular arc the optimal velocity and optimal control input are constants, we refer to the constant velocity by v_c, and consequently the optimal control input will be $u_e^{sing} = C_1 v_c^2 + C_2$. The optimal control is said to have a bang-singular-bang form as shown in Fig. 2.

Fig. 2 shows that the optimal velocity trajectory consists in general of three segments:

1. $t_0 \leqslant t \leqslant t_1$
   In the first segment where the inequality conditions in (8) hold, the optimal torque is either the maximum or the minimum. Since the initial states $(x(t_0), v(t_0))$ are specified, the initial values of costates $(\lambda_1(t_0), \lambda_2(t_0))$ are open, according to the theory of calculus of variations. A relationship between t_1 and v_c can be obtained by solving,
   $$t_1 - t_0 = \int_{v(t_0)}^{v_c} \frac{dv}{(u_e - C_1 v^2 - C_2)}$$
   Also d_1 is the area under the velocity curve and therefore can be analytically related to v_c.
2. $t_1 \leqslant t \leqslant t_2$
   This period exists only if a singular arc is determined to be a part of the optimal solution. We have shown in Appendix A that the velocity will be constant on a singular arc, therefore $v(t_1) = v(t_2) = v_c$ and $d_2 = (t_2 - t_1) v_c$. The costates will also be constants as shown in Eqs. (A.1) and (A.3) in the appendix.
3. $t_2 \leqslant t \leqslant t_f$
   In the third segment, the inequality conditions hold again and the optimal input is either at its maximum or the minimum. We have the following relationship,
   $$t_f - t_2 = \int_{v_c}^{v(t_f)} \frac{dv}{(u_e - C_1 v^2 - C_2)}$$

[3] The bang–bang (pulse and glide) fuel optimal result is corroborated by the findings in recent publications, for instance in Li et al. (2015b). In Li et al. (2015b) the authors use a nonlinear engine fuel consumption map and explain that periodic switching between high (but not the maximum) engine torque and zero engine torque is more fuel economical than operating the engine at medium torque levels. Our fuel consumption model, adopted from a recently published paper (Kamal et al., 2011) is obtained by regression and relates fuel consumption rate to vehicles speed and acceleration. As a result this model has embedded in it not only the engine fuel consumption map but also the vehicles gear shift logic. The relationship between fuel rate and acceleration input of the engine in this model is linear. Therefore, with this model, the analytically calculated optimal solution is proven to switch between maximum and zero engine acceleration input at the wheel. Note that maximum engine input at the wheel does not necessarily map to maximum engine torque due to the embedded gear shift logic. Note also that our results are also limited by its affine approximation. It is however assuring to see that a similar bang–bang optimal structure was found in Li et al. (2015b) based on a nonlinear engine map.

Please cite this article in press as: Wan, N., et al. Optimal speed advisory for connected vehicles in arterial roads and the impact on mixed traffic. Transport. Res. Part C (2016), http://dx.doi.org/10.1016/j.trc.2016.01.011

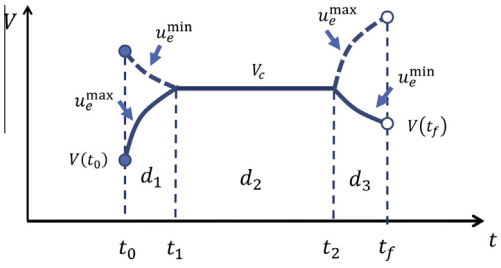

Fig. 2. The optimal strategy alternates between periods of maximum acceleration, engine shut down (or idle), and in some situations a constant speed.

The final position $x(t_f)$ is fixed, which is the position of the intersection. Therefore $\lambda_1(t_f)$ is free. The final velocity $v(t_f)$, on the other hand, can be either open or fixed. If $v(t_f)$ is open, $\lambda_2(t_f)$ should be fixed to zero according to calculus of variation theory. Given $\lambda_2(t_f) = 0$ the ordinary differential equation in Eq. (9) can be solved backward in time to find $\lambda_2(t_2)$ which is related to v_c via Eq. (A.1). This could be a tedious process and will need a numerical approach, since in Eq. (9) λ_2 and v are coupled. Alternatively if $v(t_f)$ is specified or constrained, one only needs to integrate the velocity equation and Eq. (9) does not need to be solved. This simplifies the process and allows an analytical solution to the problem. The distance d_3 is the area under the velocity curve and therefore can be analytically related to v_c.

Finally the total distance traveled is fixed and known,

$$d_1 + d_2 + d_3 = d = x(t_f) - x(t_0) \tag{10}$$

which provides an additional relationship between the unknown variables v_c, t_1, and t_2 and allows us to calculate the optimal velocity trajectory analytically.

As shown in Appendix A, only at very low speeds the constant velocity portion in segment 2 will be a part of the optimal trajectory. In the majority of scenarios the fuel optimal trajectory will be bang–bang and consists only of periods of maximum torque and glide (segments 1 and 3). Implementing this optimal solution in a real vehicle is impractical because it is both uncomfortable to the occupants and potentially disruptive to traffic. In an effort to resolve these issues, we propose to choose $v(t_f) = v_c$. By doing so, the constant speed interval extends from t_1 to t_f and the third segment can be avoided. In other words the vehicle either accelerates with maximum torque or decelerates with engine off to a constant speed and cruises past the light. We note that this choice will be sub-optimal in most scenarios, but is practical and implementable in real world conditions. By reduced idling at red lights the strategy still improves the fuel efficiency as demonstrated by the results of this paper.

The solution then reduces to the two following cases:

Case 1 : The vehicle accelerates with maximum engine torque to reach a constant speed at time t_1 as depicted in Fig. 3, therefore

$$t - t_0 = \int_{v(t_0)}^{v(t)} \frac{dv}{(u_e^{max} - C_1 v^2 - C_2)} \quad t_0 \leqslant t \leqslant t_1 \tag{11}$$

The solution is

$$v(t) = Q_1 \cdot \frac{Q_2 e^{2Q_1 C_1 (t-t_0)} - 1}{Q_2 e^{2Q_1 C_1 (t-t_0)} + 1} \quad t_0 \leqslant t \leqslant t_1 \tag{12}$$

where $Q_1 = \sqrt{\frac{u_e^{max} - C_2}{C_1}}$, $Q_2 = \left|\frac{Q_1 + v(t_0)}{Q_1 - v(t_0)}\right|$. At time t_1, the velocity reaches the constant value $v(t_1)$, which satisfies Eq. (12). The velocity trajectory should also satisfy the distance condition,

$$d = x_{t_f} - x_{t_0} = \int_{t_0}^{t_1} v(t)dt + (t_f - t_1)v(t_1) \tag{13}$$

The solution is

$$d = -Q_1(t_1 - t_0) + \frac{1}{C_1} ln\left[\frac{Q_2 e^{2Q_1 C_1 (t_1 - t_0)} + 1}{Q_2 + 1}\right] + (t_f - t_1)v(t_1) \tag{14}$$

which will be used to solve for the only remaining unknown variable t_1.

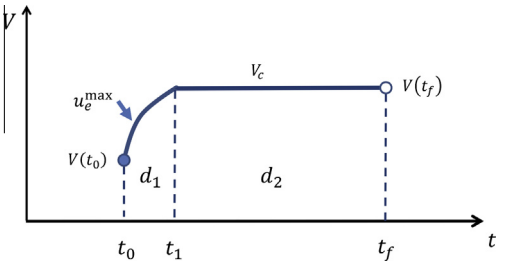

Fig. 3. A schematic of accelerate-then-cruise case.

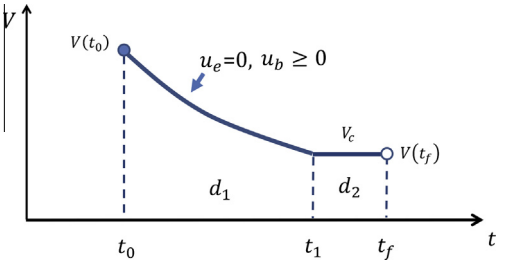

Fig. 4. A schematic of glide-then-cruise case.

Case 2 : The engine is turned off or idles with minimum torque and the vehicle decelerates to a constant speed as shown schematically in Fig. 4. There are situations when gliding alone cannot delay the vehicle enough for a green arrival. In these situations the lowest needed braking force is used to meet the boundary conditions. After introducing braking input, the vehicle longitudinal dynamics becomes:

$$\begin{cases} \dot{x} = v \\ \dot{v} = -C_1 v^2 - C_2 - u_b \end{cases} \tag{15}$$

where u_b is deceleration due to braking. Integrating the velocity equation we get:

$$v(t) = Q_3 \cdot tan[Q_4 - C_1 Q_3 (t - t_0)] \tag{16}$$

where $Q_3 = \sqrt{\frac{C_2 + u_b}{C_1}}$, $Q_4 = arctan\left(\frac{v(t_0)}{Q_3}\right)$. Integrating the velocity similar to (13), we obtain

$$d = \frac{ln[sec(-Q_4)]}{C_1} - \frac{ln[sec(C_1 Q_3 t_1 - C_1 Q_3 t_0 - Q_4)]}{C_1} + (t_f - t_1) v(t_1) \tag{17}$$

Combining Eqs. (16) and (17), there are two unknown variables u_b and t_1. For the purpose of fuel minimization, we choose the solution which gives the largest t_1 which maximizes the length of interval $[t_0, t_1]$ during which the engine is off or idling and consuming minimum fuel.

With these analytical solutions at hand, the procedure of the Speed Advisory Algorithm that we implement in our microsimulations can be summarized as follows:

Step 1: At each time step t_0, obtain the current state $(x(t_0), v(t_0))$, determine the next traffic light and obtain the position of the next upcoming light x_f.
Step 2: Assume that the vehicle accelerates to the maximum velocity and maintains the speed till it reaches the intersection. Obtain the time t_f; this is the earliest possible time the vehicle can arrive at the intersection.
Step 3: Determine whether t_f is in a green phase. If it is in a red phase, increase t_f to the beginning of the next green phase.
Step 4: Given the current vehicle speed, determine if the vehicle needs to accelerate or decelerate to arrive at position x_f at time t_f. Then use the corresponding analytical solution in Eqs. (14) or (17) to determine the velocity trajectory.
Step 5: Go back to Step 1 for next time step.

Please cite this article in press as: Wan, N., et al. Optimal speed advisory for connected vehicles in arterial roads and the impact on mixed traffic. Transport. Res. Part C (2016), http://dx.doi.org/10.1016/j.trc.2016.01.011

Note that the optimization problem is solved at every time step, so even when the vehicle motion is impeded by surrounding traffic, a new (sub)optimal velocity trajectory is obtained based on the latest position with respect to the traffic signal.

One may raise concern on the choice of t_f. In our algorithm the arrival time is set to be the earliest time the vehicle can pass the intersection, which is fixed. One may argue that choosing a later arrival time may achieve better fuel economy. While we acknowledge it, trading off travel time for one vehicle will influence other vehicles as well. Therefore we fix this condition and solve the optimal control problem based on it.

It is essential to analyze the impact of this speed advisory system, both on SAS-equipped vehicles and on other conventional vehicles in mixed traffic conditions with many vehicles. This is achieved in a microsimulation environment as described in the next section. We are interested not only in a single intersection case but also in scenarios with a series of intersections. With multiple traffic signals ahead, the optimal solution changes frequently and cannot be calculated in real time when using computationally demanding algorithms such as dynamic programming. In the following sections, we will demonstrate the advantages of the analytical SAS approach we proposed in this paper.

3. The simulation environment

Simulations are conducted in *Quadstone Paramics*^{TM}, version V6.9.3. *Paramics* is a microscopic traffic simulation software that has been widely used in academic research and commercial fields. It is capable of simulating a large number of vehicles in a wide road network and allows users to program their own functions for different types of vehicles.

The major modules used in this paper are Modeller and Programmer. Modeller is the module for traffic network model creation, simulation animation, and results storage and display. All network attributes such as road geometry, number of lanes, traffic signal timings, origins and destinations, traffic demands, vehicle types and their percentages are set in the Modeller. Programmer allows users to implement their own algorithms. Many Application Programing Interface (API) functions can be used, such as QPO (overriding existing functions), QPX (extending existing functions), QPS (setting values to variables) and QPG (getting values from variables). All APIs are written in *C* language.

In this paper, SAS is implemented in a number of vehicles by overriding their *leadspeed* and *followspeed* functions in Paramics default car following model. Our overriding function calculates and returns the reference speed at each simulation step such that idling at red is reduced. If the advised speed cannot be achieved due to other constraints, the vehicle will simply follow the speed generated by the Paramics default car-following model. After each run, all parameters such as time stamps, 3D coordinates, speed and acceleration trajectories can be stored. Fig. 5 shows a screenshot of a running simulation where conventional vehicles are in white and SAS-equipped vehicles are in green.

Next we describe the standard car following model in Paramics used by conventional vehicles and then the lane change model adopted by all vehicles is explained.

3.1. The car following model in Paramics

Paramics uses a standard car following model but enables editing several of its parameters. Each vehicle in Paramics has a target headway h. The default mean value for target headway is 1 s, however this is adjustable by the user. The value of headway of each vehicle is also affected by certain parameters such as vehicle type, heading direction, aggressiveness, and reaction time. A vehicle can operate in 3 modes: acceleration, cruising, and braking.

When the distance between the ego vehicle and the preceding vehicle exceeds a certain distance threshold, the vehicle will be in acceleration mode; the acceleration is set to be the maximum acceleration, here 2.5 m/s^2, till the ego vehicle

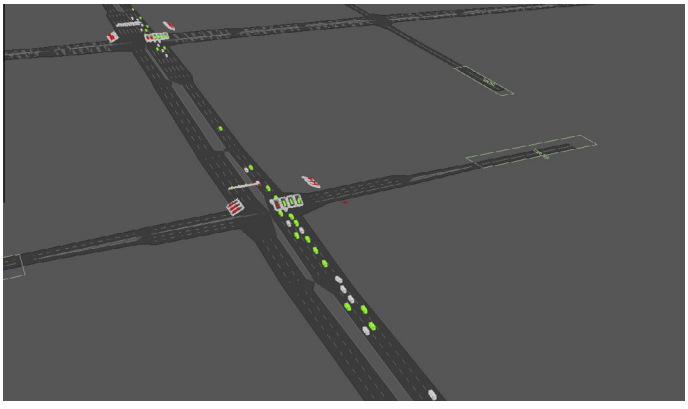

Fig. 5. A screenshot of a Paramics simulation showing SAS equipped vehicles in green and conventional vehicles in white. (For interpretation of the references to color in this figure legend, the reader is referred to the web version of this article.)

Please cite this article in press as: Wan, N., et al. Optimal speed advisory for connected vehicles in arterial roads and the impact on mixed traffic. Transport. Res. Part C (2016), http://dx.doi.org/10.1016/j.trc.2016.01.011

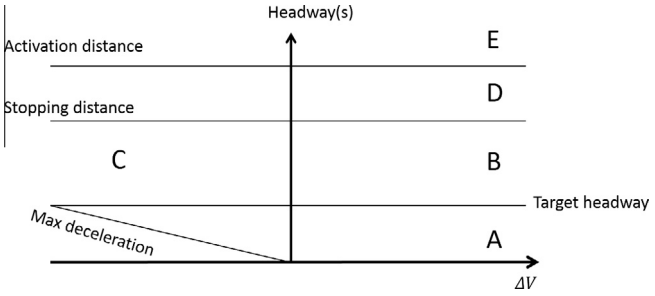

Fig. 6. Headway and velocity-difference phase space as defined in Paramics (2014).

reaches the road speed limit. When the ego vehicle detects that the preceding vehicle is braking, its acceleration is limited to a maximum of 1 m/s^2 for safety purposes.

When the distance between the ego vehicle and the preceding vehicle falls below the distance threshold, the ego vehicle will be in cruising mode. In the cruising mode, the ego vehicle tries to maintain a desired gap with the preceding vehicle, represented by s_1 and calculated as:

$$s_1 = h\Delta v \tag{18}$$

where h is the target headway and Δv is the speed difference between the ego and the preceding vehicle. In aggressive driving setting, a shorter desired gap s_2, is defined and followed:

$$s_2 = \frac{s_1^2}{d} < s_1 \tag{19}$$

where d is the current distance between the vehicles. The acceleration needed to reach the desired separation is calculated as a function of the headway and velocity difference. The headway and velocity-difference phase space is divided into several regions as shown in Fig. 6, and the acceleration in each region is calculated as follows:

$$a_A = k_1\Delta v$$
$$a_B = k_1\Delta v + k_2\frac{d - s_2}{d}$$
$$a_C = k_2\frac{d-2}{d} - \frac{(\Delta v)^2}{d - s_2}$$
$$a_D = 1\ \text{m/s}^2$$
$$a_E = 2.5\ \text{m/s}^2$$

where $k_1 = 1.0\ \text{s}^{-1}$ and $k_2 = 1.0\ \text{s}^{-2}$ are constants. More details of this policy can be found in Paramics (2014) and Duncan (1997).

3.2. The lane changing model in Paramics

Lane changing in Paramics is determined by a gap-acceptance policy, and is based on the gaps with respect to preceding and the following vehicles in adjacent lanes. Lane changing is only allowed if these gaps would be sufficiently large. Suppose Veh_0 is the vehicle that is aiming to change lane, and Veh_1 and Veh_2 are vehicles in the target lane that are in front and behind of the position Veh_0 would occupy. A lane change maneuver will happen if the following gap condition is satisfied for a period of time, typically 3–6 s:

$$g_i > \left(h_0 + \frac{\Delta v_i}{D_i} + h\right)v_i \quad i = 1, 2 \tag{20}$$

Here g_i is the gap with respect to Veh_i, h_0 is the minimum headway required for safety purposes, h is the target headway, D_i is the maximum deceleration of Veh_i, and Δv_i is the relative speed with respect to Veh_i.

4. Micro-simulation case studies

We create a number of simulation scenarios, and evaluate the impact of SAS at different congestion levels and with various penetration rates of connected vehicles. In all simulations the parameters of the vehicle longitudinal dynamics and fuel economy models are those shown in Table 1.

Please cite this article in press as: Wan, N., et al. Optimal speed advisory for connected vehicles in arterial roads and the impact on mixed traffic. Transport. Res. Part C (2016), http://dx.doi.org/10.1016/j.trc.2016.01.011

4.1. Simulation scenarios

The simulation is run in an urban corridor network. The path contains four signalized intersections. All signal timing plans are fixed and not coordinated with others. The main street has links with three or four lanes with a total length of 2.203 km (1.367 miles). The speed limit of each link is 80 km/h (49.7 mph). Conventional vehicles do not have prior access to traffic signal information and always try to reach the maximum road speed limit unless affected by nearby vehicles or traffic signals. For SAS-equipped vehicles, the minimum cruise speed is set to 2.78 m/s (10 km/h), and the maximum acceleration and deceleration are set to 2.5 m/s^2 and 2.9 m/s^2 respectively which are reasonable for passenger vehicles. Three different traffic demand levels (300, 600, and 900 vehicles per hour per lane) and seven different percentages (100%, 90%, 70%, 50%, 30%, 10%, 0%) of SAS-equipped vehicles are considered; therefore 21 simulations are conducted. Note that the results are influenced by Paramics vehicle generating model and its parameters, therefore implementing our algorithm in other simulator such as Aimsun, SUMO may provide different results.

Five main parameters of vehicles or traffic are to be statistically analyzed. We evaluate fuel consumption, acceleration, velocity, total travel time, and traffic flow. The simulation results and relational behaviors are shown next.

4.2. Simulation results

Fig. 7 compares the average individual vehicle fuel consumption for different traffic demands and percentages of SAS-equipped vehicles. It can be seen that the fuel consumption of vehicles with and without SAS are well separated,

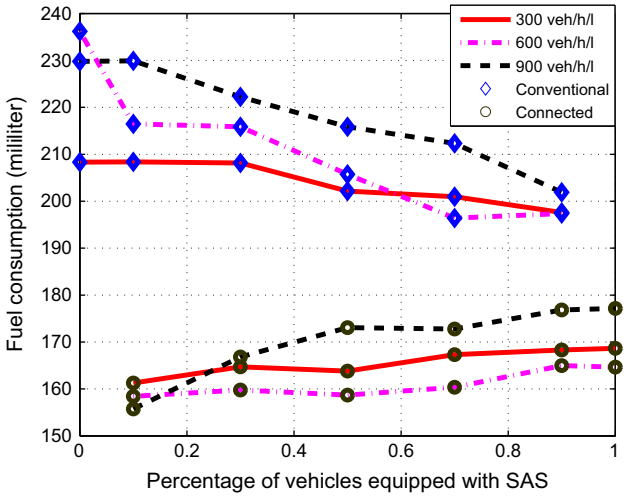

Fig. 7. Fuel consumption of vehicles with and without speed advisory system under different traffic demand levels and different penetration levels of equipped vehicles.

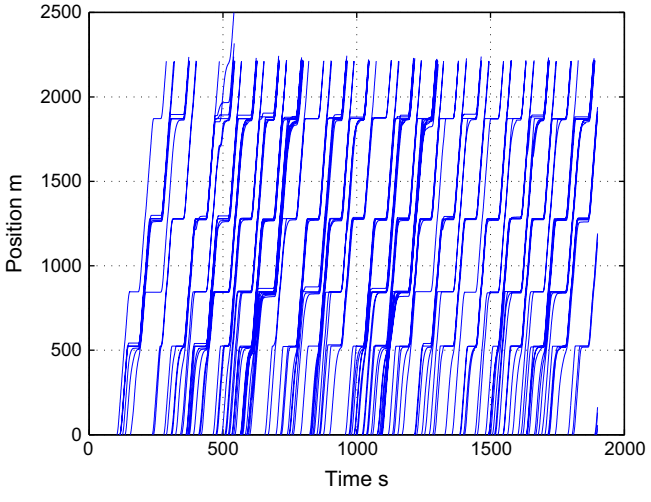

Fig. 8. Without SAS, vehicles experience more stops at each intersection.

Please cite this article in press as: Wan, N., et al. Optimal speed advisory for connected vehicles in arterial roads and the impact on mixed traffic. Transport. Res. Part C (2016), http://dx.doi.org/10.1016/j.trc.2016.01.011

SAS-equipped vehicles (three bottom curves) consume much less fuel than the ones without SAS (three top curves). This is due to fewer stops and closer to optimal operation of the engine. Another very interesting trend seen in Fig. 7 is that with the increment of the percentage of SAS-equipped vehicles, conventional vehicles consume less fuel. In other words, SAS-equipped vehicles have a positive impact on the energy efficiency of the entire mix of vehicles. With the increment of vehicles equipped with SAS, other conventional vehicles are more likely be blocked by a slower vehicle with SAS. By their simple car following strategy, such conventional vehicles may reduce the chance of stopping at intersections as well.

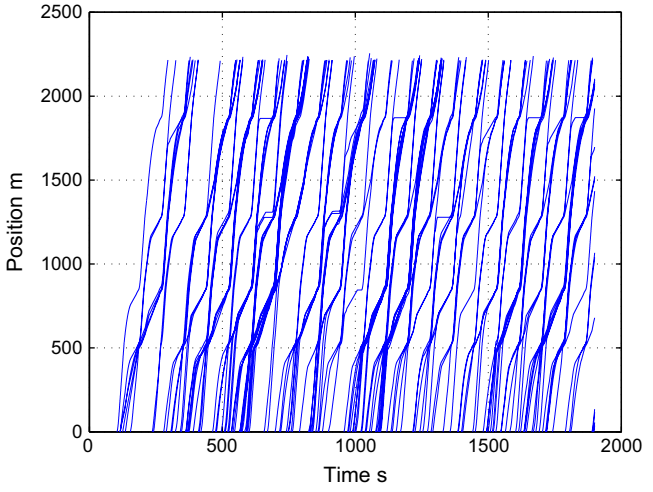

Fig. 9. Equipped with SAS, vehicles experience much fewer stops at each intersection and the trajectories are much smoother.

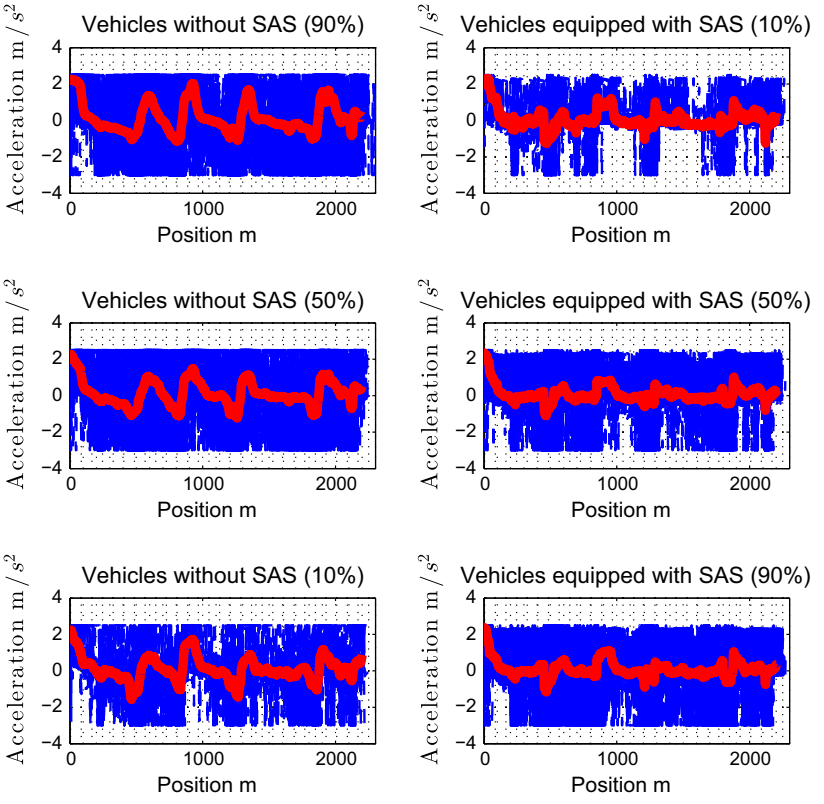

Fig. 10. Acceleration of vehicles with and without speed advisory system under 3 different penetration levels of equipped vehicles. The traffic demand was fixed at 600 veh/h/l. Accelerations of all vehicles are plotted in thin blue and the mean acceleration is plotted in thick red. (For interpretation of the references to color in this figure legend, the reader is referred to the web version of this article.)

Please cite this article in press as: Wan, N., et al. Optimal speed advisory for connected vehicles in arterial roads and the impact on mixed traffic. Transport. Res. Part C (2016), http://dx.doi.org/10.1016/j.trc.2016.01.011

The results for SAS-equipped vehicles indicate that as the traffic demand is at the demand level (900 veh/h/l), the fuel consumption of SAS-equipped vehicles is high and increases with penetration rates. It can be explained that at congested levels, slow downs and stops become more likely for all vehicles and SAS vehicles can not avoid them. It was unexpected to observe that 600 veh/h/l (mild congestion) resulted in better fuel economy than 300 veh/h/l (low congestion) for SAS vehicles. One explanation could be that in the mild congestion scenario, the vehicles are more likely to be affected by other vehicles and go at lower and more fuel efficient speeds.

In order to compare the effects of SAS, we further plot the position trajectories of multiple vehicles under same traffic conditions. Fig. 8 shows trajectories from vehicles without SAS and Fig. 9 shows trajectories from vehicles with SAS. We can clearly see that vehicles with SAS successfully avoid stops at intersections and the trajectories are much smoother.

Fig. 10 shows acceleration trajectories of all vehicles and highlights the mean acceleration over position for different penetration levels and under the same traffic demand 600 veh/h/l. Plots on the left column are of conventional vehicles, while the right column belongs to SAS-equipped vehicles. The percentage of SAS-equipped vehicles increases from top to bottom. Comparing between columns, it can be seen that the mean acceleration of SAS-equipped vehicles is significantly less than the ones without SAS. Comparing among rows, it is shown that, for vehicles with SAS, the mean acceleration does not change much. The mean acceleration of conventional vehicles without SAS on the other hand, decreases with the increment of SAS-equipped vehicles.

Note that the maximum and minimum acceleration values are sometimes above the upper limit or below the lower limit used in optimal control calculations and listed in Table 1. This is due to the fact that vehicles are interacting and when in conflict with other vehicles, a vehicle may resort to higher acceleration or lower deceleration to avoid a collision.

Fig. 11 shows velocity trajectories of all vehicles and highlights the mean velocity for different penetration levels and under the same traffic demand 600 veh/h/l. From the left column, it can be seen that the mean velocity of conventional vehicles drops at four signalized intersections. In the right column, the velocity curves are more smooth indicating that SAS-equipped vehicles react to traffic signals in advance. Similar to the acceleration plots, the mean velocity of conventional vehicles has higher fluctuations than that of SAS-equipped vehicles. And with more SAS-equipped vehicles, the mean velocity of conventional vehicles drops. These acceleration and velocity trajectories can best explain the trends observed in fuel consumption in Fig. 7.

We have thus shown that SAS-equipped vehicles improve the overall energy efficiency in mixed traffic by harmonizing the motion of conventional vehicles. This comes at a cost to overall traffic flow and vehicles' average speed. With the increment of vehicles equipped with SAS, the cumulative counts, which can be considered as average traffic flows, drop slightly. To evaluate whether such a sacrifice is acceptable, we cumulate vehicle counts for each intersection at different

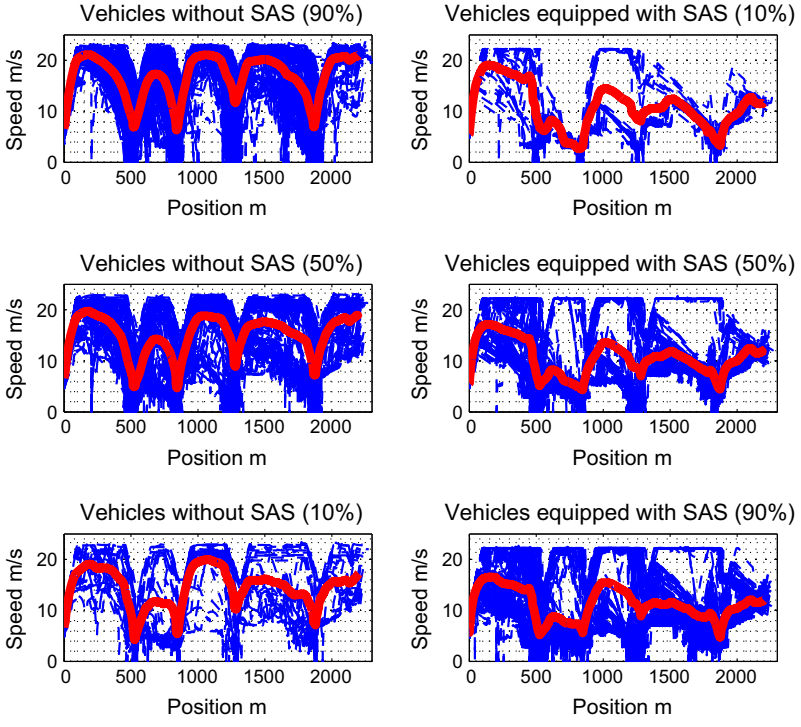

Fig. 11. Velocity of vehicles with and without speed advisory system under 3 different penetration levels of equipped vehicles. The traffic demand was fixed at 600 veh/h/l. Velocities of all vehicles are plotted in thin blue and the mean velocity is plotted in thick red. (For interpretation of the references to color in this figure legend, the reader is referred to the web version of this article.)

Please cite this article in press as: Wan, N., et al. Optimal speed advisory for connected vehicles in arterial roads and the impact on mixed traffic. Transport. Res. Part C (2016), http://dx.doi.org/10.1016/j.trc.2016.01.011

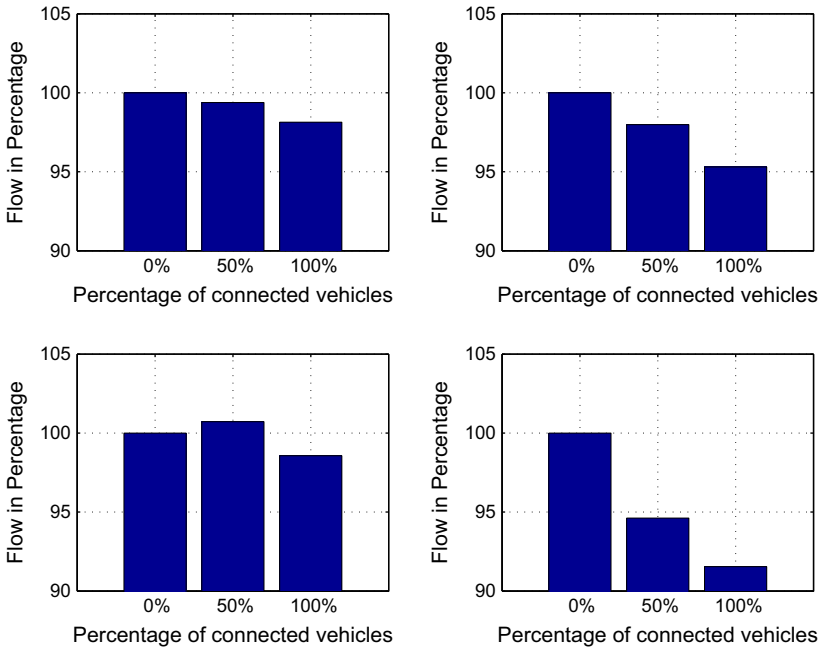

Fig. 12. Average traffic flow at four different intersections. The traffic demand was fixed at 600 veh/h/l.

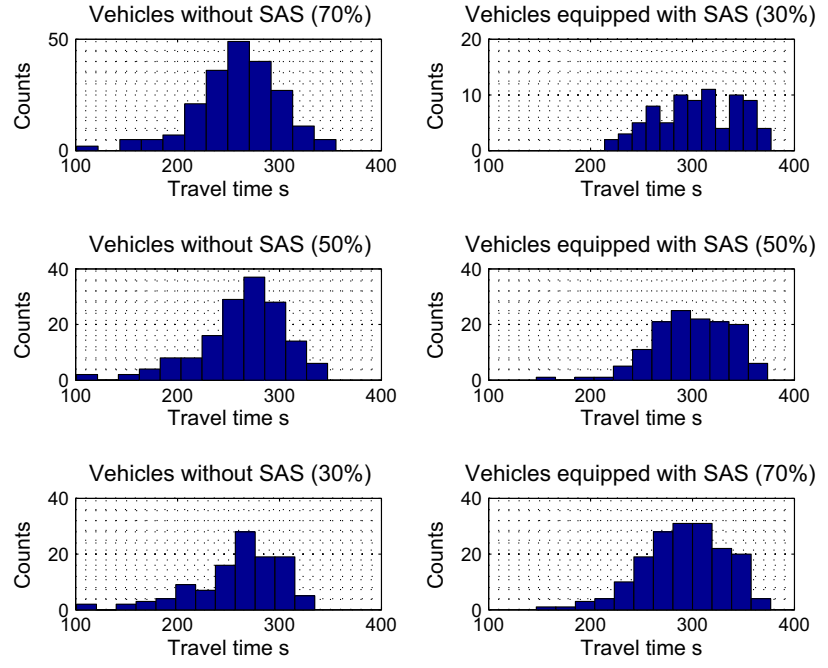

Fig. 13. Histogram of travel times for conventional and SAS equipped vehicles. The traffic demand was fixed at 600 veh/h/l.

SAS penetration rates. The vehicle counts are gathered through virtual loop detectors embedded at each simulated intersection, and the data is stored every 1 s. The traffic demand is also fixed to 600 veh/h/l. Note that at the first intersection the traffic is saturated therefore the vehicle count are similar. The remaining three intersections are not congested. Comparative plots of average traffic flow for four intersections and three SAS penetration levels are shown Fig. 12. According to these plots SAS has caused 2–8% decrease in average traffic flow. For individual vehicles this impact is best shown by observing their travel times. Fig. 13 shows travel time histograms of conventional and equipped vehicles under different SAS penetrations and when traffic demand is 600 veh/h/l. While travel time distribution of SAS-equipped vehicles remains almost the same,

that of conventional vehicles moves to the right. The mean travel time of conventional vehicles increases about 45 s, or 16%. This could be an acceptable trade-off given the benefits of much increased energy efficiency and speed harmonization.

5. Conclusion

We have shown in this paper, via 21 carefully arranged microsimulation case studies, that connected vehicles equipped with a speed advisory system have the potential to decrease their fuel consumption significantly by reducing idling at red lights. More interestingly we showed that even at relatively low penetration levels, the SAS equipped vehicles have a harmonizing effect on the motion of conventional vehicles, thus contributing to better energy efficiency of vehicles without a speed advisory system. The trade-off is a slight increase in travel times.

We formulated the speed advisory system as an optimal control problem and obtained the general structure of fuel optimal solution analytically. We demonstrated that the minimum fuel driving strategy is bang–bang in which the vehicle switches between acceleration with maximal engine torque and gliding with the engine turned off or idling until it arrives at a green light. In between these two extremes, sometimes the optimal trajectory includes periods of constant speed, but only at very low velocities. We determined that a bang–bang solution, while most energy efficient for each vehicle, would cause discomfort to the vehicle occupants and could disrupt the traffic flow. To prevent a jerky ride, we constrained the velocity to a smoother profile which was still guided by our optimal results. This solution, while suboptimal, is implementable and still increases the energy efficiency by reducing idling at traffic signals.

Acknowledgement

This research was sponsored by BMW Information Technology Research Center in South Carolina.

Appendix A. Optimal strategy on the singular interval

As shown in Eq. (8), $H_u = \partial H/\partial u$ vanishes when,

$$H_u = \beta_0 + \beta_1 v + \beta_2 v^2 + \lambda_2 = 0 \tag{A.1}$$

This relationship could only hold for a point in time, upon which the control switches between its maximum and minimum. But if this relationship holds for an interval of time, we say we have a singular interval and the optimal solution may move along a singular arc. Because the control u_e does not appear in (A.1), we cannot directly determine its optimal value on the singular arc.

However, since (A.1) must hold for an interval of time on a singular arc, its time derivatives must vanish (Bryson and Ho, 1975),

$$\frac{d^n}{dt^n}\left(\frac{\partial H}{\partial u_e}\right) = 0 \tag{A.2}$$

and it is guaranteed that upon taking time derivatives repeatedly, the control input will finally emerge and therefore can be solved for. The proof can be found in standard optimal control texts such as (Bryson and Ho, 1975).

Taking the first time derivative of Eq. (A.1) and substituting from state and co-state dynamics we get,

$$\begin{aligned}\frac{d}{dt}\frac{\partial H}{\partial u_e} &= \beta_1 \dot{v} + 2\beta_2 v\dot{v} + \dot{\lambda}_2 = 0 \\ &\Rightarrow \beta_1(u_e - C_1 v^2 - C_2) + 2\beta_2 v(u_e - C_1 v^2 - C_2) - \{\alpha_1 + 2\alpha_2 v + 3\alpha_3 v^2 + (\beta_1 + 2\beta_2 v)(u_e - C_1 v^2 - C_2) \\ &\quad + (\beta_0 + \beta_1 v + \beta_2 v^2)(-2C_1 v) + \lambda_1 - 2C_1\lambda_2 v\} = 0\end{aligned}$$

Substituting for λ_2 from Eqn. (A.1) reduces the above equation to,

$$\alpha_1 + 2\alpha_2 v + 3\alpha_3 v^2 + \lambda_1 = 0 \tag{A.3}$$

which provides a relationship between the constant co-state λ_1 and $v(t)$; but it is not still clear if this holds only at a singular point or on a singular arc. Note that u_e has not appeared in (A.3), thus we calculate the second time derivative. Since λ_1 is known to be a constant, we obtain

$$\frac{d^2}{dt^2}\frac{\partial H}{\partial u_e} = 2\alpha_2 \dot{v} + 6\alpha_3 v\dot{v} = 0 \Rightarrow (2\alpha_2 + 6\alpha_3 v)(u_e - C_1 v^2 - C_2) = 0 \tag{A.4}$$

The control input has finally appeared and when it is equal to $C_1 v^2 + C_2$ the second time derivative vanishes. If this condition holds we can also conclude that $\dot{v} = 0$ and the velocity is a constant v_c. Therefore the optimal control candidate on the singular arc is a constant and equal to:

$$u_e^{sing} = C_1 v_c^2 + C_2. \tag{A.5}$$

Please cite this article in press as: Wan, N., et al. Optimal speed advisory for connected vehicles in arterial roads and the impact on mixed traffic. Transport. Res. Part C (2016), http://dx.doi.org/10.1016/j.trc.2016.01.011

But the minimizing solution should satisfy another necessary condition referred to as Kelley's condition (Bryson and Ho, 1975) which is,

$$(-1)\frac{\partial}{\partial u_e}\left[\frac{d^2}{dt^2}\left(\frac{\partial H}{\partial u_e}\right)\right] \geqslant 0 \tag{A.6}$$

thus requiring,

$$2\alpha_2 + 6\alpha_3 v \leqslant 0 \Rightarrow v \leqslant -\frac{\alpha_2}{3\alpha_3} \tag{A.7}$$

which provides a bound on speed, above which the singular arc will not be a part of the optimal solution. In this problem and with the values listed in Table 1 the optimal solution could follow a singular arc if $v \leqslant 4.14$ m/s or 15 km/h. This is quite a low speed and therefore singular arcs of constant speed may only occasionally happen and in general the optimal solution will be of bang–bang form.

References

Asadi, B., Vahidi, A., 2009. Predictive use of traffic signal state for fuel saving. In: Proceedings of 12th IFAC Symposium on Control in Transportation Systems.
Asadi, B., Vahidi, A., 2011. Predictive cruise control: utilizing upcoming traffic signal information for improving fuel economy and reducing trip time. IEEE Trans. Contr. Syst. Technol. 19 (3), 707–714.
Au, T.-C., Zhang, S., Stone, P., May 2015. Autonomous intersection management for semi-autonomous vehicles. In: Handbook of Transportation. <http://www.cs.utexas.edu/users/ai-lab/?au:hot15>.
Bhavsar, P., He, Y., Chowdhury, M., Fries, R., Shealy, A., 2014. Energy consumption reduction strategies for plug-in hybrid electric vehicles with connected vehicle technology in urban areas. Transport. Res. Rec.: J. Transport. Res. Board (2424), 29–38.
Boyle, L.N., Mannering, F., 2004. Impact of traveler advisory systems on driving speed: some new evidence. Transport. Res. Part C: Emer. Technol. 12 (1), 57–72.
Bryson, A.E., Ho, Y.-C., 1975. Applied Optimal Control: Optimization, Estimation and Control, revised ed. CRC Press.
Duncan, G., 1997. Paramics Technical Report: Car-following, Lane-changing and Junction Modelling. Edinburgh, Scotland: Quadstone, Ltd 5(1) 5–2.
Eben Li, S., Li, K., Wang, J., 2013. Economy-oriented vehicle adaptive cruise control with coordinating multiple objectives function. Veh. Syst. Dyn. 51 (1), 1–17.
Farah, H., Koutsopoulos, H.N., Saifuzzaman, M., Kölbl, R., Fuchs, S., Bankosegger, D., 2012. Evaluation of the effect of cooperative infrastructure-to-vehicle systems on driver behavior. Transport. Res. Part C: Emer. Technol. 21 (1), 42–56.
Fayazi, S., Vahidi, A., Mahler, G., Winckler, A., 2015. Traffic signal phase and timing estimation from low-frequency transit bus data. IEEE Trans. Intell. Transport. Syst. 16 (1), 19–28.
He, X., Liu, H.X., Liu, X., 2015. Optimal vehicle speed trajectory on a signalized arterial with consideration of queue. Transport. Res. Part C: Emer. Technol. 61, 106–120.
Hellström, E., Åslund, J., Nielsen, L., 2010. Design of an efficient algorithm for fuel-optimal look-ahead control. Contr. Eng. Pract. 18 (11), 1318–1327.
Hellström, E., Ivarsson, M., Åslund, J., Nielsen, L., 2009. Look-ahead control for heavy trucks to minimize trip time and fuel consumption. Contr. Eng. Pract. 17 (2), 245–254.
Howden, C., 2015. <http://www.nhtsa.gov/About+NHTSA/Press+Releases/NHTSA-issues-advanced-notice-of-proposed-rulemaking-on-V2V-communications>.
Ioannou, P.A., Stefanovic, M., 2005. Evaluation of ACC vehicles in mixed traffic: lane change effects and sensitivity analysis. IEEE Trans. Intell. Transport. Syst. 6 (1), 79–89.
Kamal, M., Mukai, M., Murata, J., Kawabe, T., September 2010. On board eco-driving system for varying road-traffic environments using model predictive control. In: IEEE International Conference on Control Applications (CCA), 2010, pp. 1636–1641.
Kamal, M., Mukai, M., Murata, J., Kawabe, T., 2013. Model predictive control of vehicles on urban roads for improved fuel economy. IEEE Trans. Contr. Syst. Technol. 21 (3), 831–841.
Kamal, M.A.S., Mukai, M., Murata, J., Kawabe, T., 2011. Ecological vehicle control on roads with up-down slopes. IEEE Trans. Intell. Transport. Syst. 12 (3), 783–794.
Kamalanathsharma, R., Rakha, H., 2013. Multi-stage dynamic programming algorithm for eco-speed control at traffic signalized intersections. In: 16th International IEEE Conference on Intelligent Transportation Systems (ITSC), pp. 2094–2099.
Kamalanathsharma, R.K., Rakha, H.A., Yang, H., 2015. Network-wide impacts of vehicle eco-speed control in the vicinity of traffic signalized intersections. In: Transportation Research Board 94th Annual Meeting. No. 15-4290.
Katrakazas, C., Quddus, M., Chen, W.-H., Deka, L., 2015. Real-time motion planning methods for autonomous on-road driving: state-of-the-art and future research directions. Transport. Res. Part C: Emer. Technol. 60, 416–442.
Kesting, A., Treiber, M., Helbing, D., 2010. Enhanced intelligent driver model to access the impact of driving strategies on traffic capacity. Philos. Trans. Roy. Soc. Lond. A: Math. Phys. Eng. Sci. 368 (1928), 4585–4605.
Kirk, D.E., 2012. Optimal Control Theory: An Introduction. Courier Corporation.
Koukoumidis, E., Peh, L.-S., Martonosi, M.R., 2011. SignalGuru: leveraging mobile phones for collaborative traffic signal schedule advisory. In: Proceedings of the 9th International Conference on Mobile Systems, Applications, and Services. ACM, pp. 127–140.
Krueger., G., Fehr, W., 2013. Overview of the Michigan connected vehicle test bed. <http://www.its.dot.gov/testbed/PDF/2-Krueger_PlugfestIntro%20.pdf>.
Li, S., Hu, X., Li, K., Ahn, C., 2015a. Mechanism of vehicular periodic operation for optimal fuel economy in free-driving scenarios. Intell. Transp. Syst. IET 9 (3), 306–313.
Li, S., Peng, H., June 2011. Strategies to minimize fuel consumption of passenger cars during car-following scenarios. In: American Control Conference (ACC), 2011, pp. 2107–2112.
Li, S.E., Deng, K., Zheng, Y., Peng, H., 2015b. Effect of pulse-and-glide strategy on traffic flow for a platoon of mixed automated and manually driven vehicles. Comput.-Aided Civ. Infrastruct. Eng. 30 (11), 892–905.
Li, S.E., Peng, H., Li, K., Wang, J., 2012. Minimum fuel control strategy in automated car-following scenarios. IEEE Trans. Veh. Technol. 61 (3), 998–1007.
Mahler, G., Vahidi, A., 2014. An optimal velocity-planning scheme for vehicle energy efficiency through probabilistic prediction of traffic-signal timing. IEEE Trans. Intell. Transport. Syst. 15 (6), 2516–2523.
Mandava, S., Boriboonsomsin, K., Barth, M., 2009. Arterial velocity planning based on traffic signal information under light traffic conditions. In: 12th International IEEE Conference on Intelligent Transportation Systems, 2009, ITSC'09. IEEE, pp. 1–6.
Manzie, C., Watson, H., Halgamuge, S., 2007. Fuel economy improvements for urban driving: hybrid vs. intelligent vehicles. Transport. Res. Part C: Emer. Technol. 15 (1), 1–16.
Mensing, F., Bideaux, E., Trigui, R., Ribet, J., Jeanneret, B., 2014. Eco-driving: an economic or ecologic driving style? Transport. Res. Part C: Emer. Technol. 38, 110–121.

Please cite this article in press as: Wan, N., et al. Optimal speed advisory for connected vehicles in arterial roads and the impact on mixed traffic. Transport. Res. Part C (2016), http://dx.doi.org/10.1016/j.trc.2016.01.011

Ozatay, E., Onori, S., Wollaeger, J., Ozguner, U., Rizzoni, G., Filev, D., Michelini, J., Di Cairano, S., 2014. Cloud-based velocity profile optimization for everyday driving: a dynamic-programming-based solution. IEEE Trans. Intell. Transport. Syst. 15 (6), 2491–2505.

Ozatay, E., Ozguner, U., Onori, S., Rizzoni, G., 2012. Analytical solution to the minimum fuel consumption optimization problem with the existence of a traffic light. In: ASME 2012 5th Annual Dynamic Systems and Control Conference joint with the JSME 2012 11th Motion and Vibration Conference. American Society of Mechanical Engineers, pp. 837–846.

Paramics, 2014. The Paramics Manuals. QuastoneParamics.

Rakha, H., Kamalanathsharma, R.K., 2011. Eco-driving at signalized intersections using V2I communication. In: 14th International IEEE Conference on Intelligent Transportation Systems (ITSC), 2011. IEEE, pp. 341–346.

Vahidi, A., Stefanopoulou, A., Peng, H., 2005. Recursive least squares with forgetting for online estimation of vehicle mass and road grade: theory and experiments. Veh. Syst. Dyn. 43 (1), 31–55.

Wollaeger, J., Kumar, S., Onori, S., Filev, D., Ozguner, U., Rizzoni, G., Di Cairano, S., June 2012. Cloud-computing based velocity profile generation for minimum fuel consumption: a dynamic programming based solution. In: American Control Conference (ACC), 2012, pp. 2108–2113.

Xia, H., Boriboonsomsin, K., Barth, M., 2013. Dynamic eco-driving for signalized arterial corridors and its indirect network-wide energy/emissions benefits. J. Intell. Transport. Syst. 17 (1), 31–41.

Xia, H., Boriboonsomsin, K., Schweizer, F., Winckler, A., Zhou, K., Zhang, W.-B., Barth, M., September 2012. Field operational testing of eco-approach technology at a fixed-time signalized intersection. In: 15th International IEEE Conference on Intelligent Transportation Systems (ITSC), 2012, pp. 188–193.

Please cite this article in press as: Wan, N., et al. Optimal speed advisory for connected vehicles in arterial roads and the impact on mixed traffic. Transport. Res. Part C (2016), http://dx.doi.org/10.1016/j.trc.2016.01.011